

1

2 **Case study**3 **Intrahepatic multicystic biliary hamartoma: presentation of a case report and magnetic**4 **resonance imaging / magnetic resonance cholangiopancreatography findings**

5

6

7 **Abstract :** Biliary hamartomas, known as von Meyenburg complexes (VMCs), are benign
8 liver malformations. They are histologically characterized by cystic dilated bile ducts
9 surrounded by numerous fibrous stromal elements measuring up to 5 mm in diameter.
10 Incidental detection of VMCs by autopsy is difficult. Detection of VMCs by imaging is also
11 difficult because of their asymptomatic nature and small size and also rarity. Moreover, they
12 are easily confused with metastatic diseases of the liver, especially in imaging .

13 A 39-year-old man presented to our hospital with a 6-month history of recurrent nonspecific
14 abdominal pain. Abdominal ultrasonography (US) revealed multiple cystic lesions in the liver
15 that appeared to be metastases. However, final diagnosis was VMCs. This case report
16 highlights the routine differential diagnosis of biliary microhamartomas by magnetic
17 resonance imaging and magnetic resonance cholangiopancreatography.

18

19 **Key words :** biliary microhamartomas, magnetic resonance imaging (MRI), magnetic
20 resonance cholangiopancreatography (MRCP)

21 **Introduction**

22

23 Biliary hamartomas, known as von Meyenburg complexes (VMCs), are benign liver
24 malformations. They are histologically characterized by cystic dilated bile ducts surrounded
25 by numerous fibrous stromal elements [1,2] measuring up to 5 mm in diameter. Incidental

detection of VMCs by autopsy is difficult. Detection of VMCs by imaging is also difficult because of their asymptomatic nature and small size [3]. VMCs are also rare. Moreover, they are easily confused with metastatic diseases of the liver, especially in imaging [4].

Therefore, an understanding of the imaging traits of VMCs is needed to establish a list of differential diagnoses, which will decrease the need for methods such as biopsy or laparotomy [5]. We herein report a case of VMCs and describe the routine diagnostic magnetic resonance imaging (MRI) and magnetic resonance cholangiopancreatography (MRCP) findings of biliary microhamartomas.

Case report

A 39-year-old man presented to our hospital with a 6-month history of recurrent nonspecific abdominal pain. Physical examination findings were unremarkable. Laboratory examination results were normal with the exception of a slight elevation of gamma-glutamyl transferase (142 mg/dL; reference range, 0–55 mg/dL). Abdominal ultrasonography (US) revealed multiple cystic lesions in the liver that appeared similar to metastases. Subsequent MRI showed multiple small cysts that were hypointense on T1-weighted images (Fig. 1a, b) and hyperintense on T2-weighted images; they were scattered in the liver parenchyma (Fig. 2a, b). MRCP showed small cysts distributed uniformly within the contour of the liver, creating a “starry sky” configuration (Fig. 3a, b).

The patient was diagnosed with multiple VMCs based on the typical MRI features. Verification using these imaging techniques within the 6-month follow-up confirmed the diagnosis of VMCs.

Discussion

A VMC is a benign congenital malformation of the biliary duct. It was first defined in 1918 by von Meyenburg [6]. Although jaundice and portal hypertension may be caused by a mass effect, patients are usually asymptomatic [7]. VMCs may be single or multiple, with sizes ranging from 1 to 15 mm [1]. Because of the small size of the lesions, an ultimate description is difficult to attain.

The prevalence of VMCs by autopsy ranges from 0.6% to 2.8% [8]. Histologically, the lesions include disorganized and dilated bile ducts and ductules surrounded by fibrous stroma [9]. US imaging shows hypoechoic, hyperechoic, or mixed heterogenic echoic structures [1,3,4]. The multiple comet-tail sign is considered to be a specific US finding of VMCs [3]. Additionally, lesional echogenicity might be related to the number and size of dilated bile ducts and the degree of fibrosis [9]. In contrast, enhanced computed tomography shows that VMCs are usually of low attenuation with irregular margins. Most reported cases have suggested that VMCs do not demonstrate contrast enhancement [3,9]. On MRI, VMCs are defined as hypointense on T1 and hyperintense on T2 compared to the surrounding liver parenchyma [1,9].

Although VMCs are benign, some reports have described hepatic malignancies with a background of VMCs, including hepatocellular carcinoma and cholangiocarcinoma [10]. VMCs are rare and usually only seen as multiple small nodules. They are sometimes confused with metastatic liver disease, microabscesses, diffuse primary hepatocellular carcinoma, biliary cysts, or Caroli disease [1,6,8].

Conclusion

The use of various imaging modalities with follow-up has proven helpful for the diagnosis of VMCs. A correct diagnosis is easier to reach when typical imaging findings are present. Otherwise, histological verification may be needed.

References

1. Lev-Toaff AS, Bach AM, Wechsler RJ, Hilpert PL, Gatalica Z, Rubin R. The radiologic and pathologic spectrum of biliary hamartomas. *AJR Am J Roentgenol* 1995; 165: 309-313

- 97 2. Wei SC, Huang GT, Chen CH, Sheu JC, Tsang YM, Hsu HC, Chen DS. Bile duct
98 hamartomas. A report of two cases. J Clin Gastroenterol 1997; 25: 608-611
- 99 3. Luo TY, Itai Y, Eguchi N, Kurosaki Y, Onaya H, Ahmadi Y, Niitsu M, Tsunoda HS. Von
100 Meyenburg complexes of the liver: imaging findings. J Comput Assist Tomogr 1998; 22: 372-
101 378
- 102 4. Cooke JC, Cooke DA. The appearances of multiple biliary hamartomas of the liver (von
103 Meyenberg complexes) on computed tomography. Clin Radiol 1987; 38: 101-102
- 104 5. Mortelé B, Mortelé K, Seynaeve P, Vandewelde D, Kunnen M, Ros PR. Hepatic bile duct
105 hamartomas (von Meyenburg Complexes): MR and MR cholangiography findings. J Comput
106 Assist Tomogr 2002; 26: 438-443
- 107 6. Zheng RQ, Zhang B, Kudo M, Oanda H, Inoue H. Imaging findings of biliary
108 hamartomas. World J Gastroenterol, 2005; 13(40):6354-6359.
- 109 7. Wohlgemuth WA, Bottger J, Bohndorf JB. MRI, CT, US and ERCP in the evaluation of
110 bile duct hamartomas (von Meyenburg complex): A case report. Eur Radiol, 1998; 8:1623-
111 1626.
- 112 8. Markhard BK, Rubens DJ, Huang J, Dogra VS. Sonographic Features of Biliary
113 Hamartomas with Histopathologic Correlation. J Ultrasound Med, 2006; 25:1631-1633.
- 114 9. Yong Moon Shin. Biliary hamartoma presented as a single mass. The Korean Journal of
115 Hepatology, 2011; 17:331-334.
- 116 10. Maher MM, Dervan P, Keogh B, Murray JG. Bile duct hamartomas (von Meyenburg
117 complexes): Value of MR imaging in diagnosis. Abdominal Imaging, 1999; 24:171-173.
118
119
- 120 Figure 1A: T2-weighted three-dimensional magnetic resonance cholangiopancreatography
121 images (coronal plane). Multiple hyperintense cysts with scattered placement are observed in

122 the liver parenchyma, the largest diameter reaching about 2 cm. No significant association
123 between the cysts and biliary ducts is present.

124 Figure 1b: T2-weighted three-dimensional magnetic resonance cholangiopancreatography
125 images (coronal plane). Multiple hyperintense cysts with scattered placement are observed in
126 the liver parenchyma, the largest diameter reaching about 2 cm. No significant association
127 between the cysts and biliary ducts is present.

128

129 Figure2a :T1-weighted contrast-enhanced axial fat-suppressed sequences. (a, b) Multiple
130 hypointense cysts, the largest of which is 2 cm in diameter, are observed in the liver
131 parenchyma without contrast enhancement.

132 Figure 2b :T1-weighted contrast-enhanced axial fat-suppressed sequences. (a, b) Multiple
133 hypointense cysts, the largest of which is 2 cm in diameter, are observed in the liver
134 parenchyma without contrast enhancement.

135 Figure 3a :Multiple hyperintense cysts in the liver parenchyma. (a) Coronal-plane T2-
136 weighted sequence, (b) axial fat-suppressed T2-weighted sequence

137 Figure 3b: Multiple hyperintense cysts in the liver parenchyma. (a) Coronal-plane T2-
138 weighted sequence, (b) axial fat-suppressed T2-weighted sequence.

139

140

141



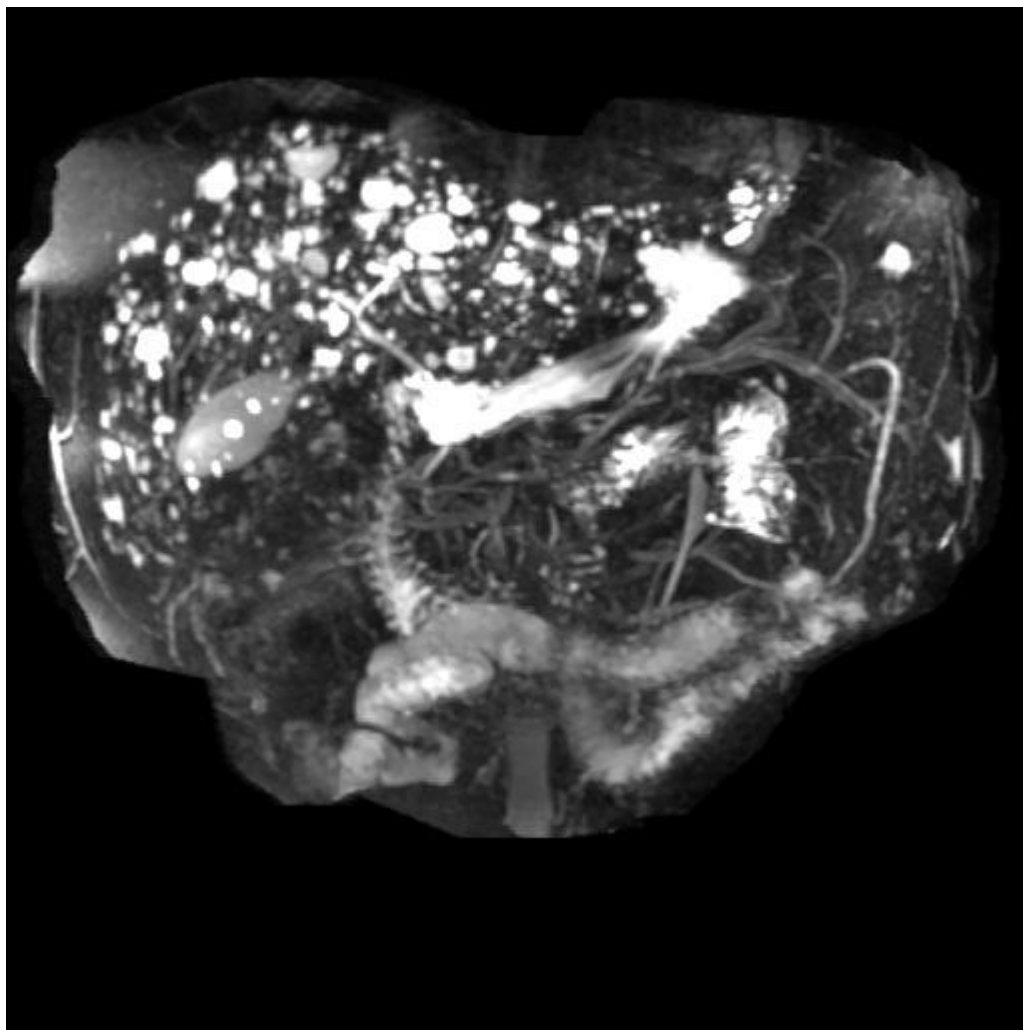
142

143

144

145

Figure1A



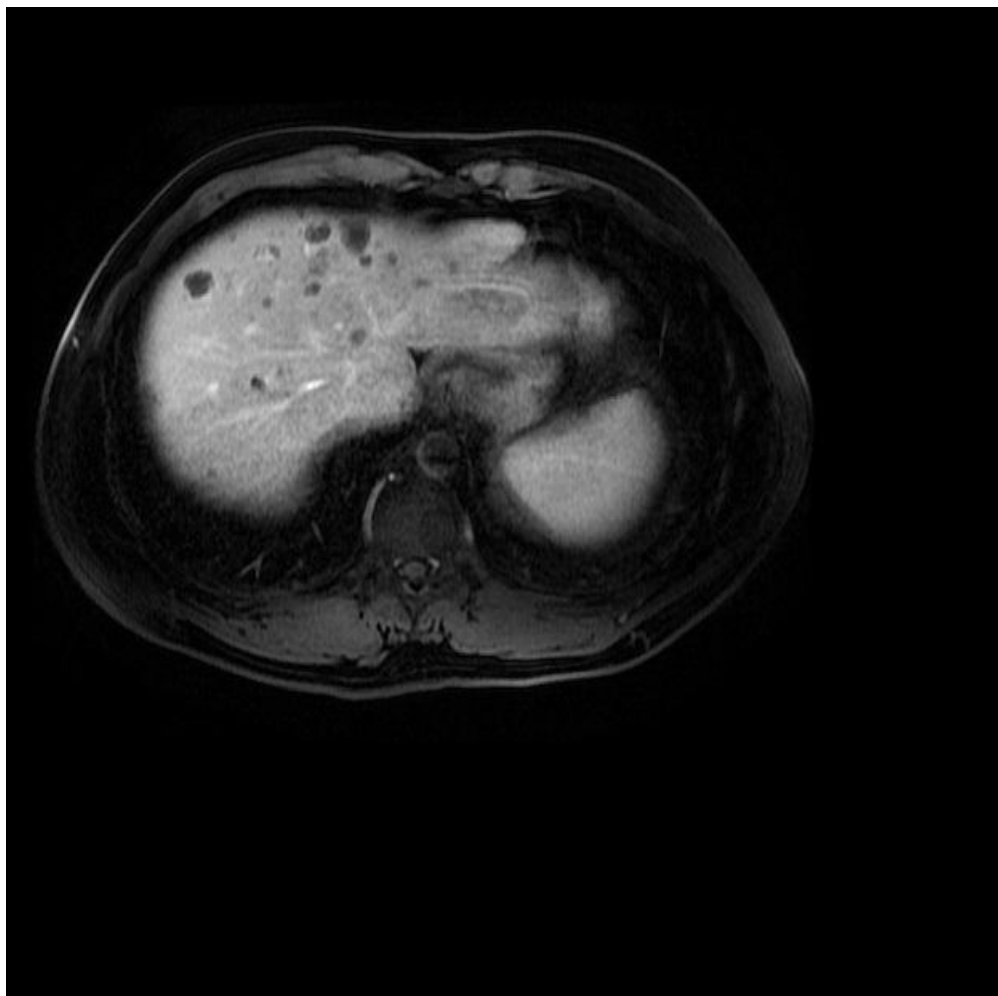
146

147

148

Figure 1b

149



150

151 Figure2a

152

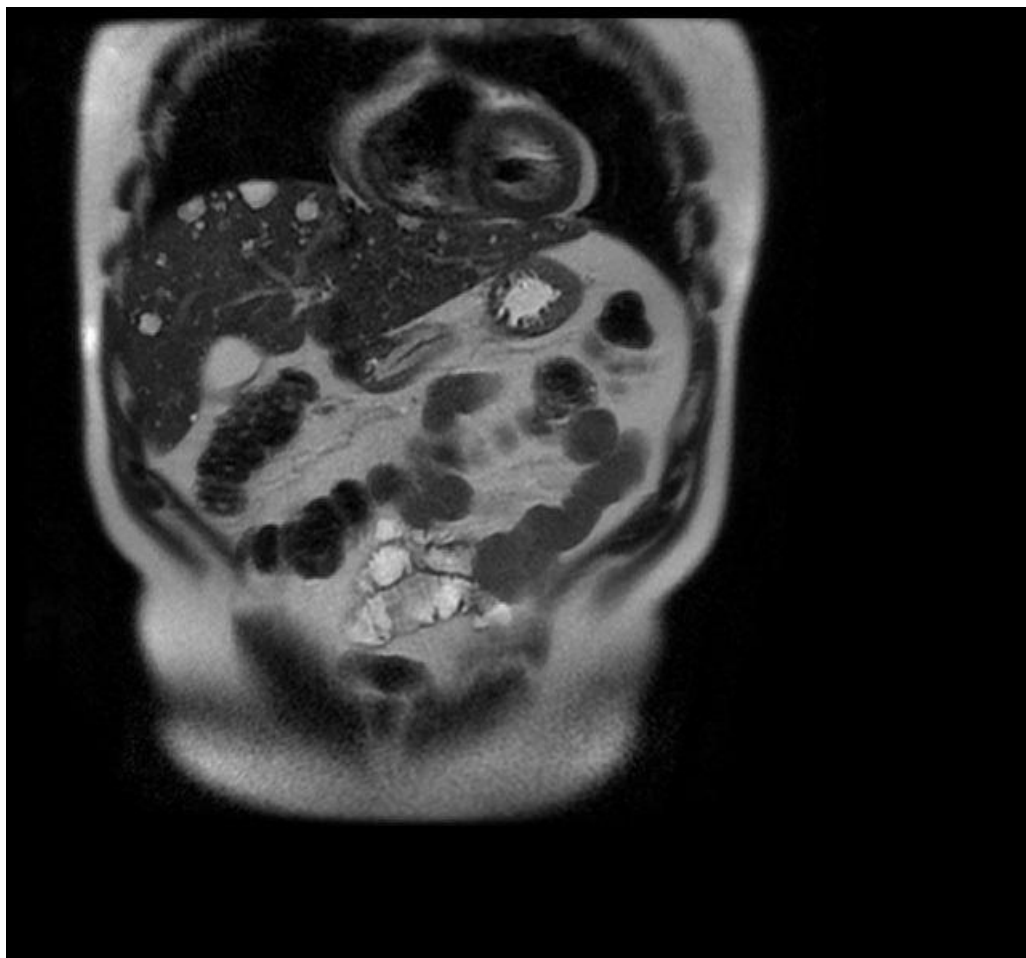


153

154

155 Figure 2b

156



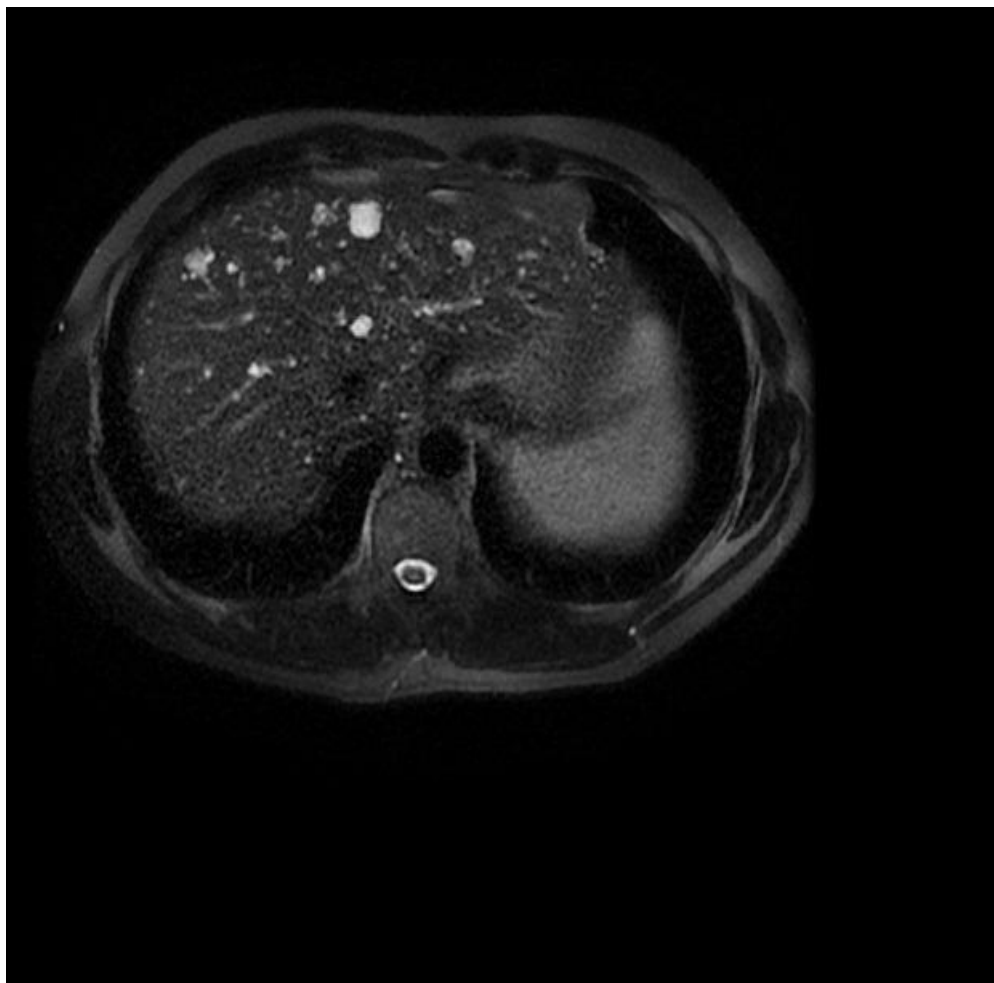
157

158

159

Figure 3a

160



161

162

163

164

Figure 3b